Nordic Optical Telescope Scientific Association

Technical report

DEFORMATION CALCULATIONS

of

the primary and secondary mirrors of

the Nordic 2.5 m optical telescope

Torben E. Andersen

Niels Chr. Jessen

March 1985

CONTENTS

1. INTRODUCTION

The Nordic 2.5 m optical telescope is presently being designed and is planned to go into operation in 1988. It will be an alt/az telescope for Cassegrain operation and it will be placed in a co-rotating building.

The telescope is conceived with cost savings in mind. The main mirror will be fast, f/2, which leads to a short telescope tube. Furthermore, the main mirror is thin, with an aspect ratio of 13.5. The mirror therefore has low weight and the telescope structure can be rather light.

The use of a fast, thin mirror has important advantages. However, the design of the main mirror cell becomes more critical and a thorough structural analysis of the optics is necessary. Such an analysis has been performed using the finite element method and the results are presented in this report.

The correct procedure for calculations of this type would be first to calculate the mirror deformations using a finite element program and secondly to do ray-tracing on the basis of the deflection pattern to determine image quality. It is however time-consuming to perform ray-tracing for every single finite element run. It has therefore been chosen to perform the finite element calculations with the simple criterion that peak-to-peak surface errors (that cannot be focused out or do not correspond to tilt) should not significantly exceed 60 nm. Later, a separate ray-tracing is then required to show that the support configuration selected actually does give an acceptable optical quality.

The finite element calculations have been performed using the computer program NASTRAN. This program is one of the most powerful FEM-programs existing today. It has numerous facilities, among which the restart capability and the contour plotting option are of particular importance for the present application.

2. MAIN MIRROR

The geometry of the main mirror is shown on figure 1. It is made of Zerodur, its mass is calculated to be 1925.999 kg and its center of gravity to lie 77.1 mm above the bottom plane.

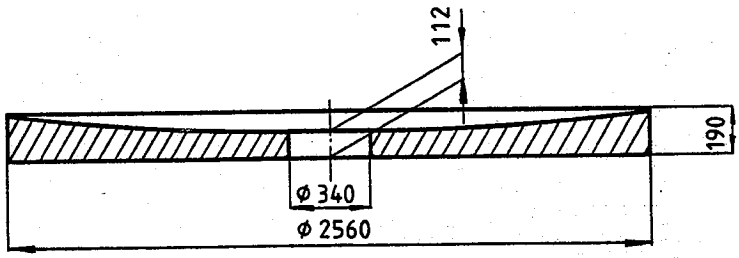

Fig.1. Main mirror geometry.

The analysis of the deflection pattern of the main mirror has been performed using two different finite element models. The first model is an axisymmetric one which requires only limited computing power to solve the equations. This model was used for determination of the diameters of the support rings and as an independent check of the results of the larger 3-D model. The second model, the 3-D model, was used to determine all other load deformation patterns.

In the following, the two models are described separately.

2.1 Axisymmetric Model

The axisymmetric model was formulated using 8x30 hexagonal, solid elements as shown in figure 2. The mirror is supported at 3 circular knife-edges that constrain the axial movement of the

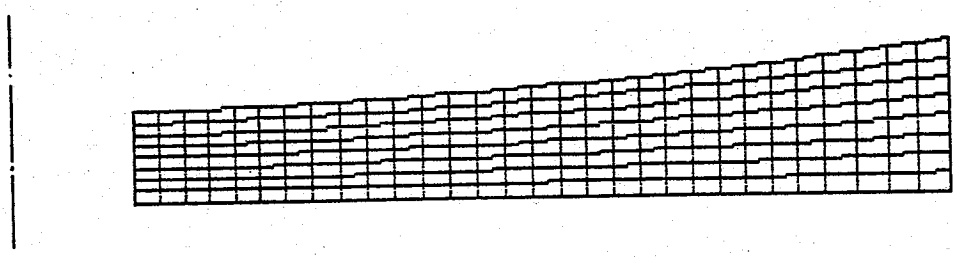

Fig. 2. Section of axisymmetric mirror model.

mirror to zero at the support rings. It is desirable both to have nodes at the position of the support rings and to be able to perform the deflection calculations for arbitrarily selected ring diameters. For this reason it is necessary to do modifications in the grid pattern when the support diameters are varied in the

calculations. To accomplish this in a simple way, a preprocessor was programmed to generate the NASTRAN input data automatically on the basis of given mirror dimensions and support ring diameters.

A number of runs were performed to determine the best ring diameters. The best one was obtained with the choice of diameters for which results are shown in the figures 3 and 4. Figure 3

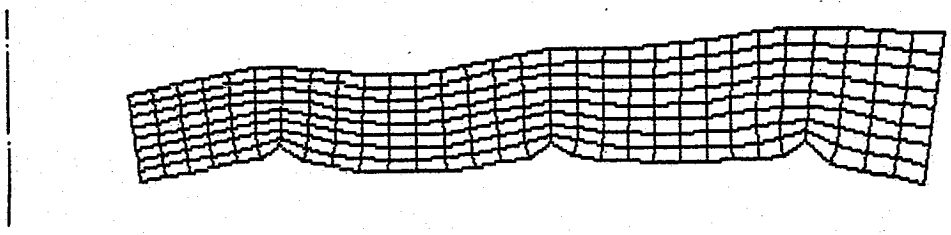

Fig. 3. Deformation pattern of axisymmetric model.

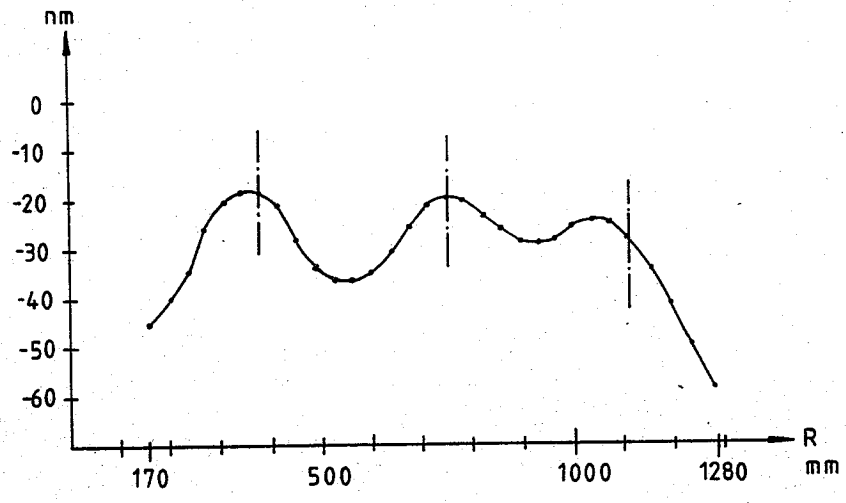

Fig. 4. Deformations of axisymmetric model.

shows the mirror section with magnified deformations and figure 4 the actual deformations. The deflections essentially stay within ±10 nm, with the exception of the inner and outer rims of the mirror that have larger deflections. It should be noted that the innermost and outermost part of the mirror is not used for optical purposes.

A marginal improvement in the deflection pattern could possibly still be obtained by performing more runs and continuing the optimization process further. However, with the present support diameters the deflections are so small that is was decided to stop at this point.

From the axisymmetric calculations it may be concluded that the following ring diameters and ring loads are near-optimal:

Ring diameter	Ring load
750 mm	13.61%
1500 mm	29.18%
2220 mm	57.21%

The indicated ring diameters have actually been selected for the cell. The ring loads have not been adopted exactly as indicated, since engineering requirements do not permit a totally free selection of these loads. Further comments on this will be given in the next chapter.

2.2 3-Dimensional Model

A 3-D model is required to study the influence of the transverse supports and the discrete axial supports. Such a model has been formulated in NASTRAN and is shown in figure 5 and 6.

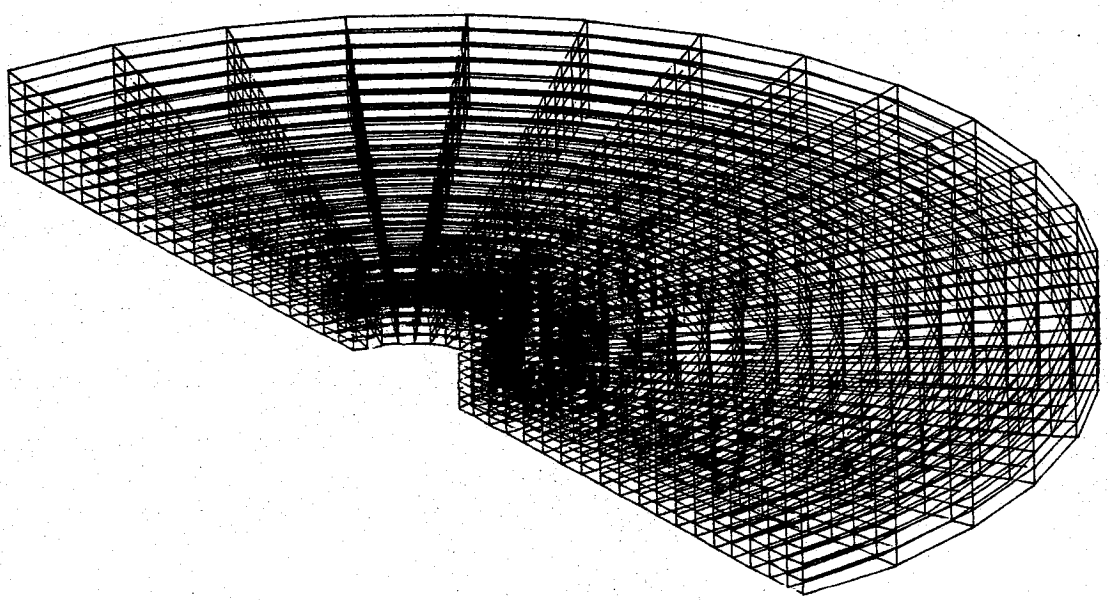

Fig. 5. 3-D finite element model of main mirror.

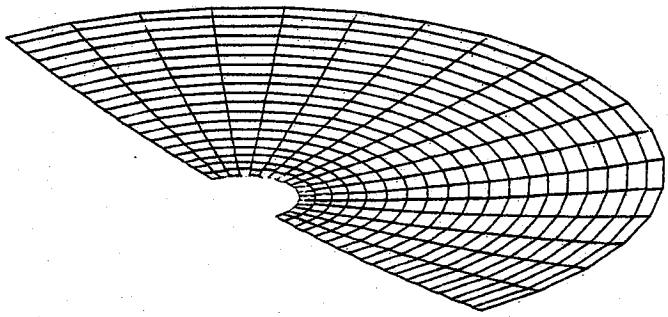

Fig. 6. Top surface of 3-D model.

The model describes 180 degrees of the mirror, thus enabling both the influence of the transverse and the axial supports to be studied by use of the same model. The model has 6 layers of hexagonal elements each corresponding to a mirror sector of 10 degrees. The model has been generated using the MsgMESH preprocessor. There are 2052 hexagonal elements and 2660 grid points.

By the calculations related to this model, extensive use has been made of the restart capability of NASTRAN. In this way, is has not been required to perform the stiffness matrix inversion for every load case. This was done once and for all and the intermediate results were stored on a disk file and used for each new load case.

Axial Supports. Axial support systems have traditionally been designed with counterweighted lever arms. The tolerance on the force exerted by each support has usually been very tight (0.1-1%), since accumulated errors of the support forces otherwise produce considerable load errors on the 3 defining points. The present 2.5 m mirror is very thin and a large number of axial supports is therefore necessary. For this mirror the tolerance on the support forces would be exceptionally tight and a counterweighted system would be costly.

It was therefore decided to adhere to another solution, namely to use electronically controlled air pistons and defining points with load cells. The forces of the support pads are thus controlled in such a way that the defining points do not carry any significant load. The defining points do therefore not deform or support the mirror and their location can be chosen freely.

The "air pistons" have been designed by means of metallic bellows arranged as shown in figure 7. The supports are placed in

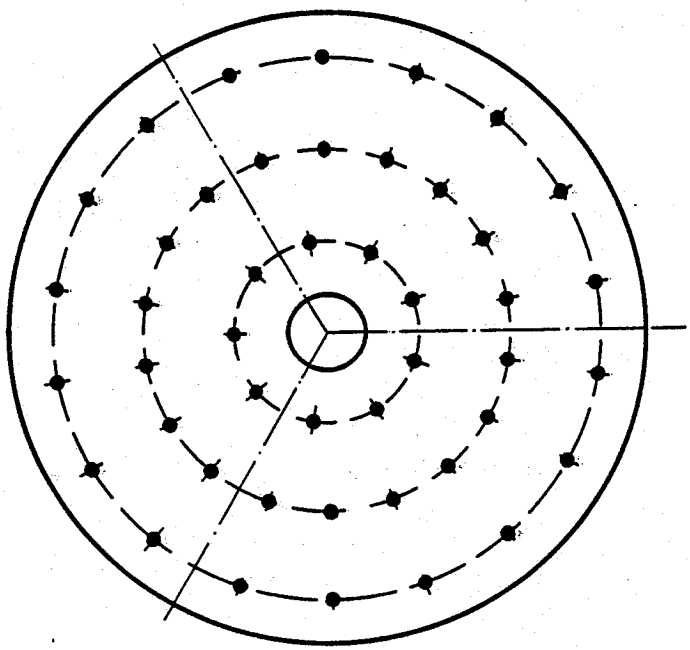

Fig. 7. Axial support configuration.

3 rings with the diameters determined in section 2.1 and with a tangential spacing which is roughly equal to the distance between the rings. For control purposes there must be a 120 degrees rotational symmetry, for which reason the number of supports in each ring must be multiples of 3. Also, it is desirable to use identical support pads, at least for the two inner rings. The choice of the support pads and their number therefore poses a design puzzle. The system selected and shown on figure 7 is a good compromise that fulfils all of the above mentioned requirements. There is a small disadvantage due to the fact that outer ring supports are located at the same angular position as the middle ring supports, but the deformation calculations (to be presented below) show that this does not lead to any significant image degradation.

The deformation pattern corresponding to a pure axial gravity load is shown on the contour plot of figure 8.

The load distribution actually selected is

Ring diameter	Ring load
750 mm	14.00%
1500 mm	28.01%
2200 mm	57.99%

As a result of a minor programming error, all contours are double, showing deformations both on the top and in a layer slightly below the surface. The computing cost of removing the extra contours would be high and it was therefore decided to let them stay in this and all of the other computer runs with the 3-D model.

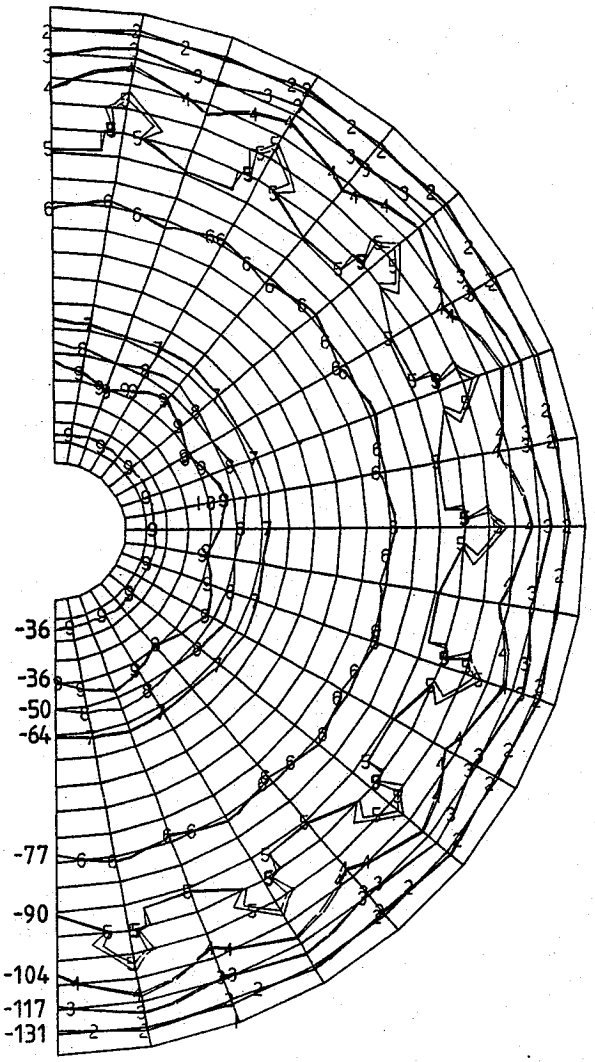

Fig. 8. Contour plot of axial deformations due to axial support system when pointing to zenith. Deflections are in nm.

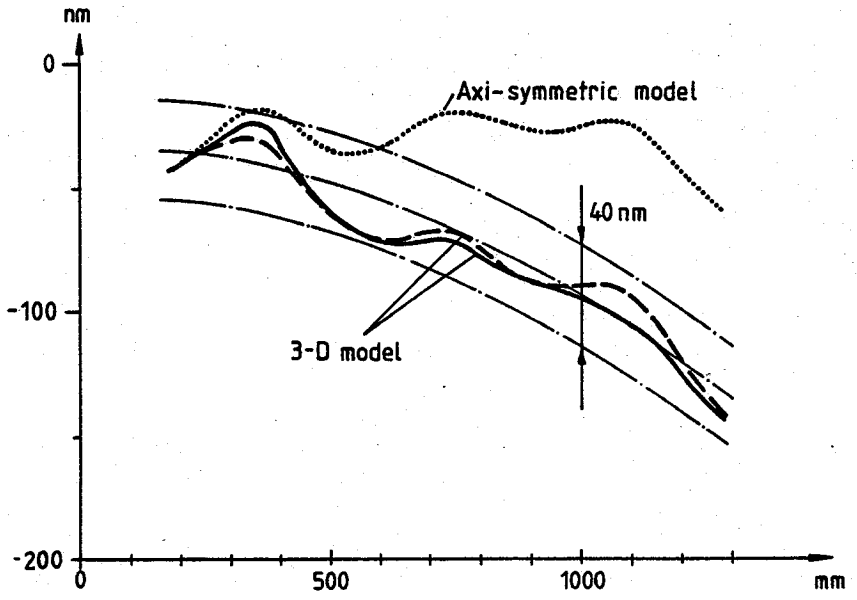

Fig. 9. Comparison of results from 3-D model to results from axisymmetric model. Difference is due to different ring loads.

In figure 9 the axial deformation as a function of radius has been drawn. The dashed curve corresponds to a radial section through support points of outer and middle rings. The solid curve corresponds to a section through supports of the inner ring. It is seen that they only deviate little from each other.

The dotted curve of figure 9 shows the deflection determined by means of the axisymmetric model described in chapter 2.1. It is seen that there is a difference between the results of the two models. This difference does not stem from model inaccuracies, but from the fact that the ring loads have been slightly modified to fulfil the above described engineering requirements. Changes in the ring loads produce "coning", an effect which best can be compared with the deflection of a Belleville washer.

The coning of the mirror is here of the order of 100 nm at the mirror edge. This coning can be focused out to the extent shown by the parabolic curves of figure 9. The corresponding axial focusing movement of the secondary is about 7 μm when changing from observations near zenith to observations near the horizon. This movement is insignificant as compared to other deformations in the telescope structure. The coning corresponds to a change in image scale of $6.2 \cdot 10^{-7}$ mm/arcsec and this change is not critical for the guiding capability of the telescope.

The three axial defining points can be designed in two different ways. According to a first principle, the defining point permanently carries a small, insignificant load, say 1 kp, and always detects positive forces. The second principle employs an average load of zero, but the defining point must then be able to carry both positive and negative forces, i.e. the defining pad must be glued to the mirror.

It is from an engineering point of view attractive to choose the first solution, since the pad then need not be glued to the mirror. To study the feasibility of this principle, two load cases were run on the computer with three defining point forces of 1 kp, but without gravity load. The results are shown

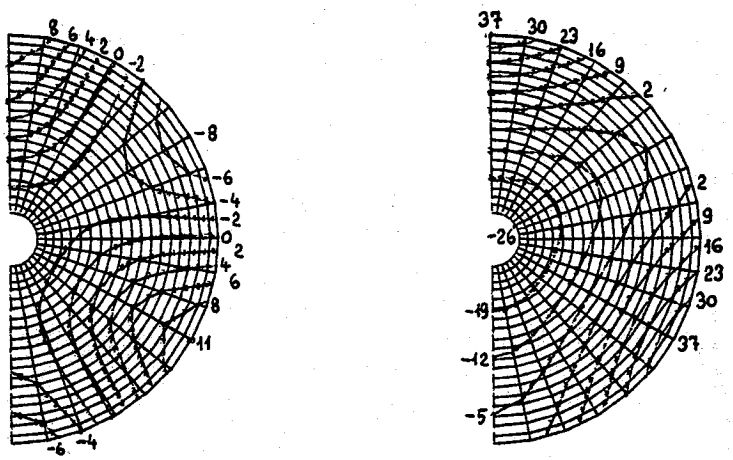

Fig. 10. Deflection patterns from defining point forces of 1 kp. Deflections are in nm.

in figure 10. It is seen that the deformations in neither case are ignorable and for the case with defining points near the edge, the deformations are too high. It was however found advantageous to locate the defining points near the edge, where cell deformation is negligible, and it was therefore decided to opt for zero-force defining points with pads glued to the mirror. As a consequence of the above calculation, it may be seen that the zero offset in the air regulator system should be below 0.05-0.1 kp load on each defining point.

The metallic bellows used for axial supports each have a certain weight. A part of this weight will occur as a transverse load that will be carried by friction between the bellows and the mirror cell. This load will again be taken by the two transverse defining points on the side of the mirror (see also next chapter). The worst-case mirror deformation due to this load is shown on figure 11. It is seen that the deformation is harmless, especially because a part of the deformation corresponds to a tilt of the mirror.

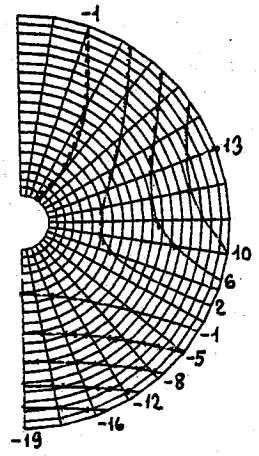

Fig. 11. Deformations due to transverse load from axial supports. Deflections are in nm.

The metallic bellows each have a certain effective cross section which multiplied by the pressure above atmosphere inside the bellows determines the force of the support pad. Due to a uniform production process, the bellows are identical to a very high precision. However, since the outer ring bellows are bigger than the bellows of the two inner rings, it is possible that the ratios between the effective cross sections of the two sizes of bellows are not exactly as indicated by the manufacturer. To study the consequence of this effect, three computation runs were performed with an 1-percent overload on respectively the inner, the middle and the outer support ring. The results are shown in figure 12. It may be seen that errors in the ring loads lead to the coning described earlier. This coning can largely be focused out and is not critical provided that any ring overload does not exceed 1%.

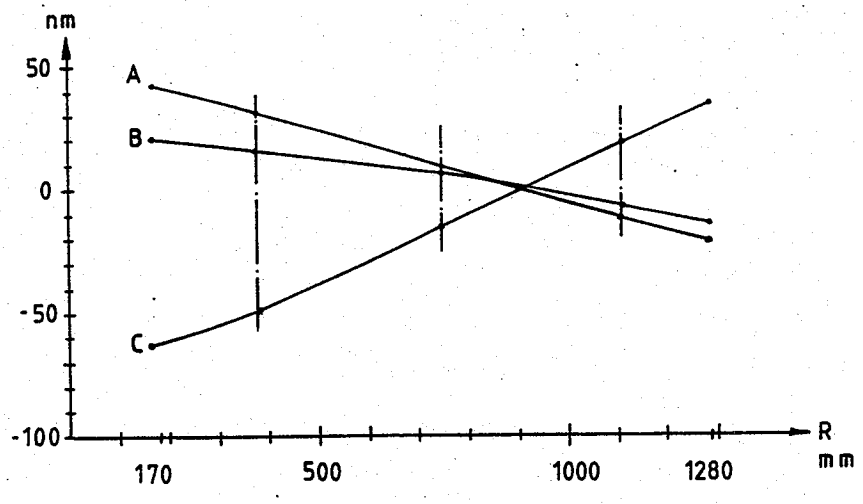

Fig. 12. A: 1% overload at inner ring, B: 1% overload at middle ring, C: 1% overload at outer ring.

Tolerances on the ring diameters have not been determined using the 3-D model. However, experience from the axisymmetric calculations shows that a normal machine shop tolerance (say ±0.5 mm) will be more than sufficient for the ring diameters.

Transverse Supports. Since metallic bellows are used as axial supports, it would be attractive to also make use of such ones for the transverse supports. However, it is not simple to design a bellows-support that is capable of pulling on the upper edge of the mirror. As a consequence, a transverse support system with metallic bellows seems most feasible if it is a push-only system on the lower edge of the mirror. A computer calculation was performed to see if such a system could be used. The deformations were found to be far too large and consequently the thought of a push-only transverse support system was dropped and it was decided to use lever arms with counterweights.

The traditional push-pull systems employ a cosine force distribution along the periphery and the forces are always perpendicular to the mirror edge. Such a system is the obvious choice for an equatorially mounted telescope. However, for an alt/az telescope a cosine system exerts unnecessarily large forces to the edge of the mirror. For such a telescope, it is more reasonable to apply a pure transverse support system as the one shown in figure 13.

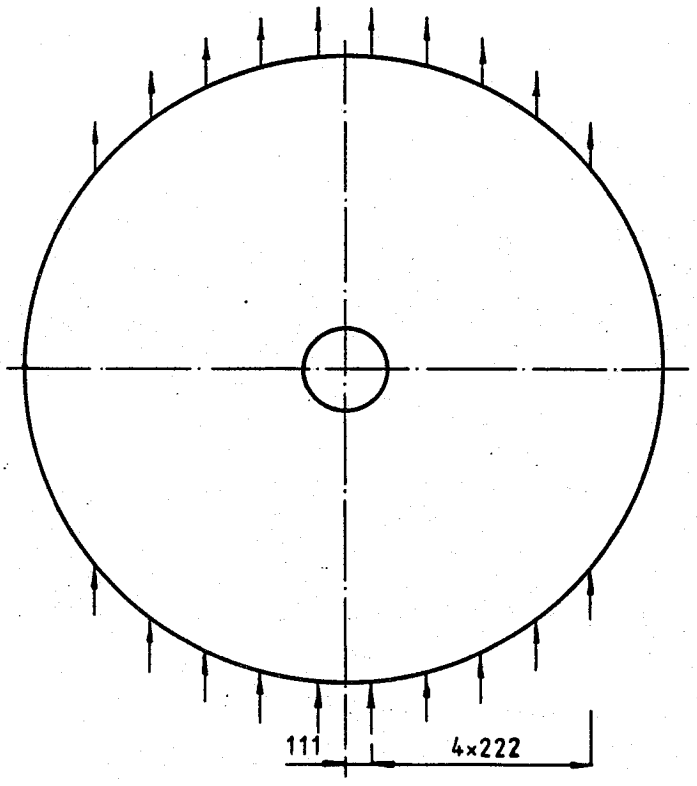

Fig. 13. Transverse push/pull support configuration.

The free design parameters are

- Number of supports
- Forces of supports
- Location of supports

The number of supports was chosen to be 5 in each quadrant. This initial guess was essentially based upon experience from other telescopes, but the calculations to be presented later in this chapter have confirmed the feasibility of using this number of supports. It is possible that 4 supports would be sufficient, but the cost of calculations to prove it, would far exceed the cost of the few extra supports.

The support forces were selected all to be equal, since this simplifies the mechanical design. The distances between the individual supports are also equal. No attempt has been made to vary and optimize these forces and distances since satisfactory results were obtained with the constant values.

It is imperative that the resultant of the transverse support forces go through the center of gravity of the mirror. A calculation of the deformation pattern corresponding to a load case where all of the support forces lie in a plane through the center of gravity revealed too large deflections (of the order of ±70 nm). For instance, at the lower edge the "overhang" of the mirror makes the mirror retract at that location as seen from the reflecting side of the mirror.

To compensate for this overhang, the transverse supports have been offset axially as shown on figure 14. This is similar

Fig. 14. Axial positions of transverse supports.

to the principle originally proposed by D. Brown in (1), but the supports are here displaced in a direction opposite to the one suggested by D. Brown. The resulting deflections are shown in the contour plot of figure 15. The deflections are about ±40 nm which

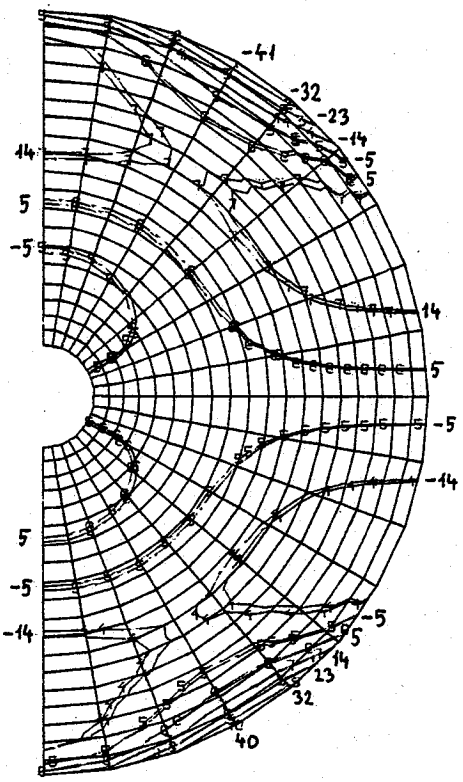

Fig. 15. Deformations from transverse supports with telescope pointing to the horizon. Deflections are in nm.

is acceptable, since

1) a part of the deflections correspond to mirror tilt and

2) the specifications of image quality when pointing near the horizon are more relaxed than those at zenith.

Figure 16 depicts the same situation except for the fact, that the mirror has been displaced 1 mm axially with respect to the transverse supports. As a consequence, the resulting transverse force does not anymore go through the center of gravity, but has an offset of 1 mm.

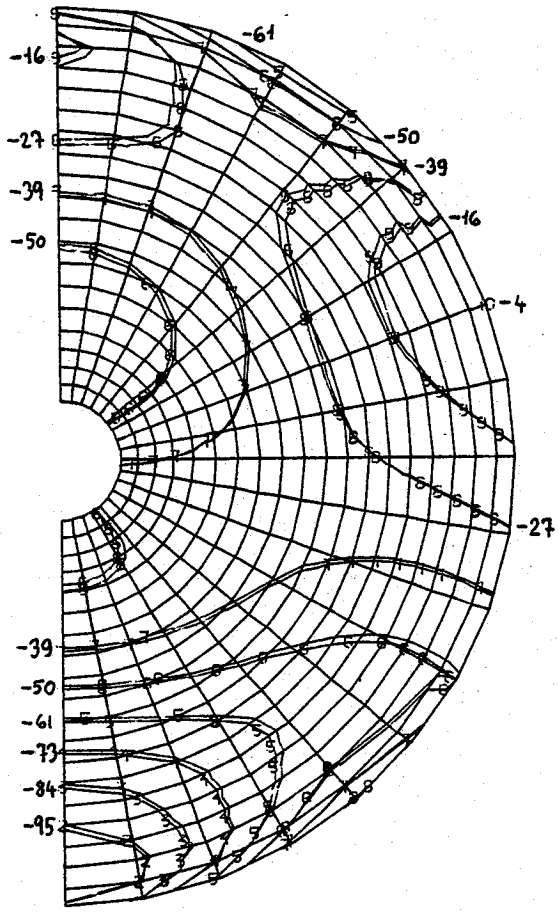

Fig. 16. Deformations from transverse supports with the main mirror displaced 1 mm axially in its cell. Deflections are in nm.

The axial deformations are now higher and it may be concluded that the resulting transverse force should not be offset by more than about 0.5 mm from the center of gravity of the mirror. In other words, the axial position of the mirror in its cell should be correct to within 0.5 mm.

Figure 17 shows the situation when the load on single pad

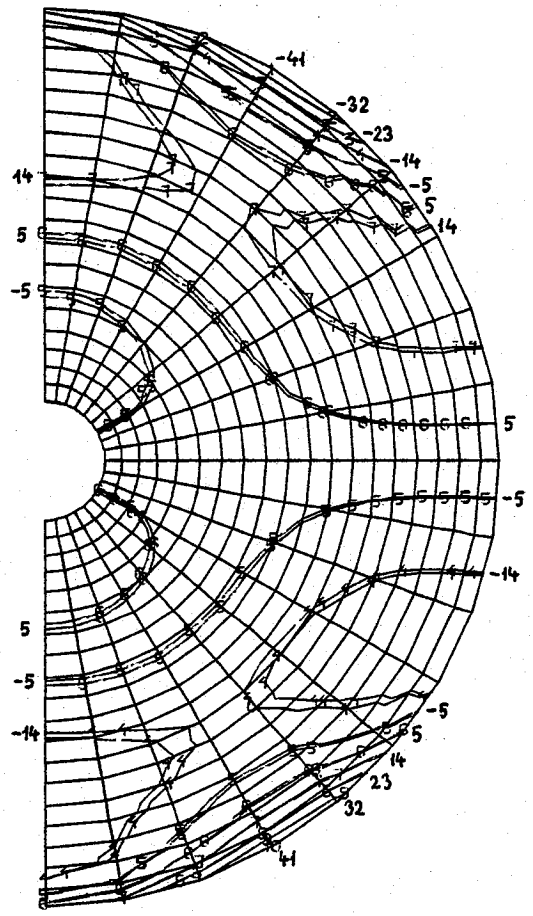

Fig. 17. Deflection pattern with 0.5% underload on lower left pad. Deflections are in nm.

is decreased by 0.5%. The corresponding underload is taken by a defining point on the side of the mirror in the cog-plane. There is no significant change in the deflection pattern as compared to the ideal case of figure 15. Consequently a 1% tolerance on the transverse load forces is safe.

Combined Load. The image quality specification remains constant from zenith to an altitude of 30 degrees, from where it is relaxed. It is therefore of interest to study the combined load case corresponding to 30 degrees' altitude. The contour plot for this load case is shown on figure 18. The deflections are within ±50 nm. This value includes both coning (that can be focused out) and tilt (that does not degrade image quality significantly). The deflection pattern is therefore fully acceptable.

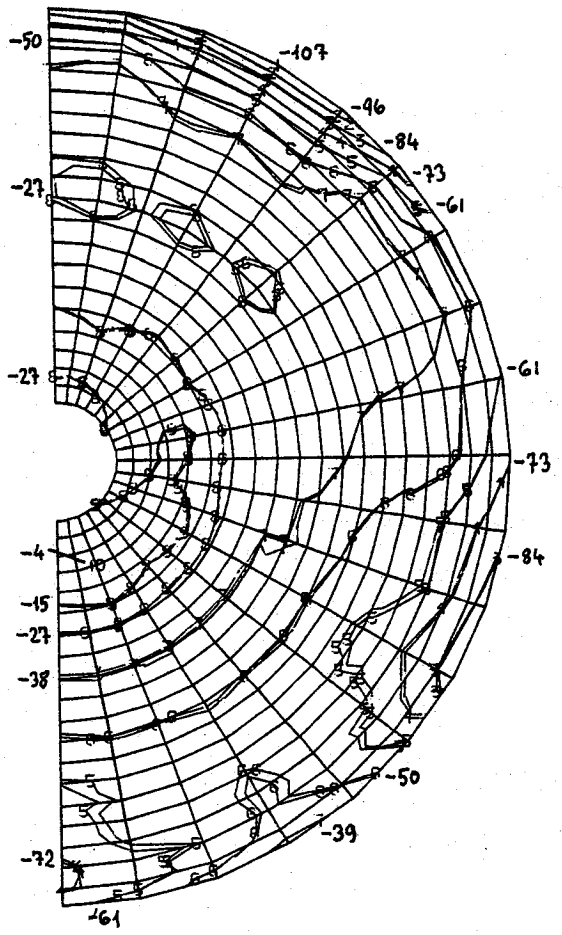

Fig. 18. Deflection pattern with telescope pointing to an altitude of 30 degrees. Deflections are in nm.

3. SECONDARY MIRROR

The geometry of the secondary mirror is shown on figure 19. The mirror is made of Zerodur and it has a mass of 45.687 kg. The center of gravity lies 47.84 mm under the flat top plane.

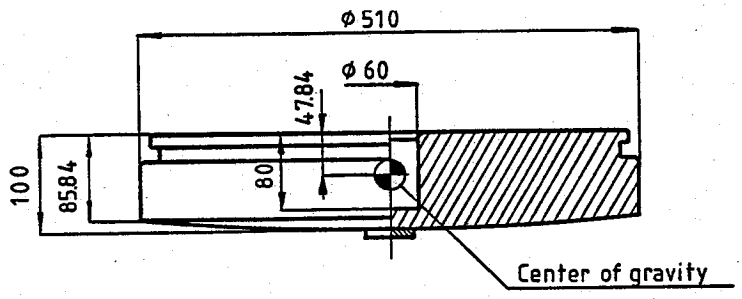

Fig. 19. Secondary mirror geometry.

The mirror deformations were also for this mirror determined by means of the finite element program NASTRAN. Two models were formulated. The first one is axisymmetric and suitable for calculating axisymmetric deflections due to axisymmetric loads. It has the advantage of being inexpensive in computer-time. The second model is a 3-D model which can be used for any arbitrary load. This model is more expensive in use.

3.1 Axisymmetric Model

The axisymmetric model (see figure 20) basically has 423 nodes and 181 elements. However, during the calculations, different mirror geometries have been tested and the precise number of nodes and elements have therefore been varied from calculation to calculation.

It was originally the intention to use a mirror with a thickness of 80 mm. The axisymmetric model therefore describes such a mirror. During the subsequent 3-D modelling, the mirror thickness was increased to 100 mm. It was however for cost reasons decided not to renew the axisymmetric calculations with the thicker mirror.

The axisymmetric calculations do therefore not precisely describe the performance of the mirror that was actually chosen but are anyway presented here, since they, in a valuable way, add to the insight in the support problem.

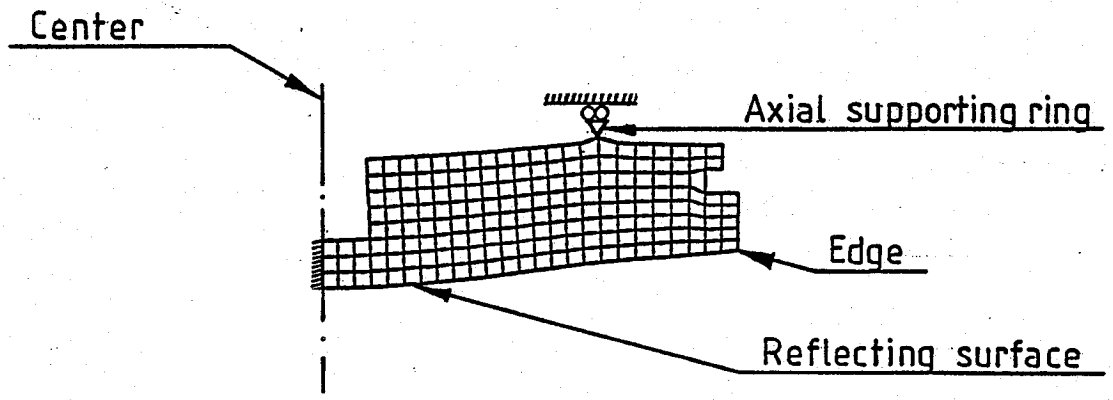

Fig. 20. Deformation pattern of axisymmetric model.

Axial Support. The axial support system will have a number of pulling "piano-wires" fixed to the upper side of the mirror and arranged in a ring. The design problem is to determine the numbers of wires that are required and the diameter of the ring.

The axisymmetric model provides for an efficient means for determining the optimal ring diameter. The model was constrained to simulate a mirror fixed to a pulling "knife-edge" on the flat top side. The optimal diameter was determined using the criterion that the displacements in the center and at the edge of the reflecting surface should have the same value. With a radius of 160-170 mm the criterion was fulfilled. The displacements have a value of ±7 nm. An example of a deformed model is shown in figure 20.

Thermal Expansions. The secondary mirror will be supported laterally through a hole in the center. It must be assured that this transverse system does not produce erroneous forces or moments.

Two designs have been considered. The first one is of the ball-bearing type and the second one of the membrane type.

The first design is shown in figure 21. The balls are placed between two ground surfaces and there is a certain preload to take out play. The outer ring is bonded to the mirror.

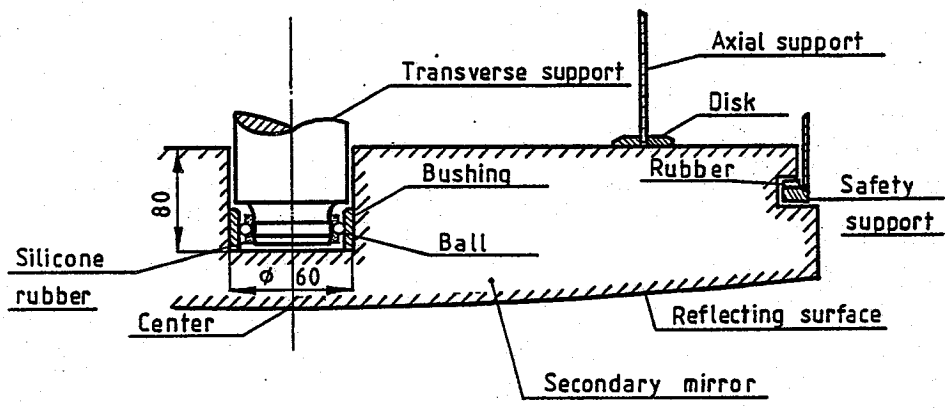

Fig. 21. Support system. For the final transverse support system membranes are selected instead of balls.

The ring expands when the temperature rises (see figure 22). Since the mirror does not expand, the bushing will load the mirror radially. The bushing must be of hardened steel to avoid local plastic deformation at the ball contact points. A low-expansion steel alloy, such as Invar, can not be hardened and can therefore not be used for this application.

The radial mirror loading during operation is proportional to the difference between the operation temperature and the temperature at which the ring was bonded into the mirror hole. The radial mirror loading is therefore minimized by bonding the ring into the mirror at the average temperature of operation. It is anticipated that the maximum difference between this bonding temperature and the temperature of operation does not exceed 20°C and that value has been used for calculations of the mirror deformations due to thermal loading.

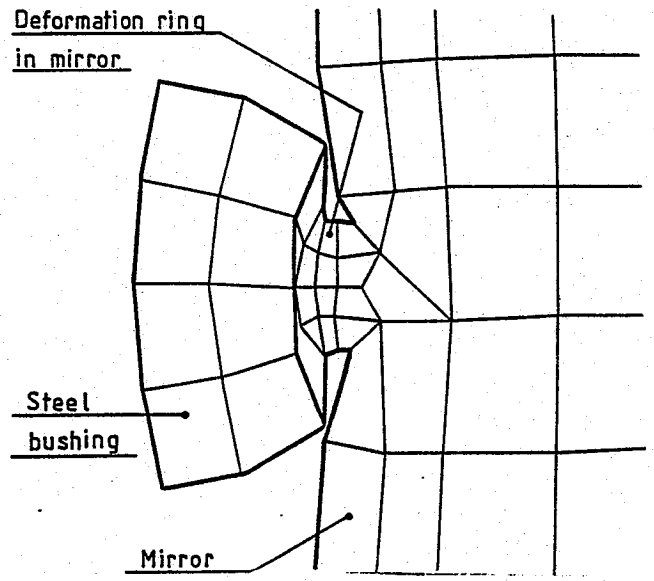

Fig. 22. Expanded steel bushing with exaggerated deformations.

With a steel-bushing as shown on figure 21 the displacements on the reflecting surface are ±640 nm. To obtain smaller displacements using a steel ring there are four ways to go:

1) Decrease thickness of bushing.

2) Decrease the height of bushing.

3) Decrease diameter of bushing.

4) Alter geometry of secondary mirror.

A substantial number of calculations were performed but it is not possible to get deflections below ±72 nm by combining the four solutions. The displacements become too big and can not be tolerated. The conclusion is that ordinary steel can not be used as material for the bushing and the ball bearing principle was therefore rejected for this application.

The second design, which was actually chosen, uses membranes to connect the bushing and the inner cylindrical part (see figure 23).

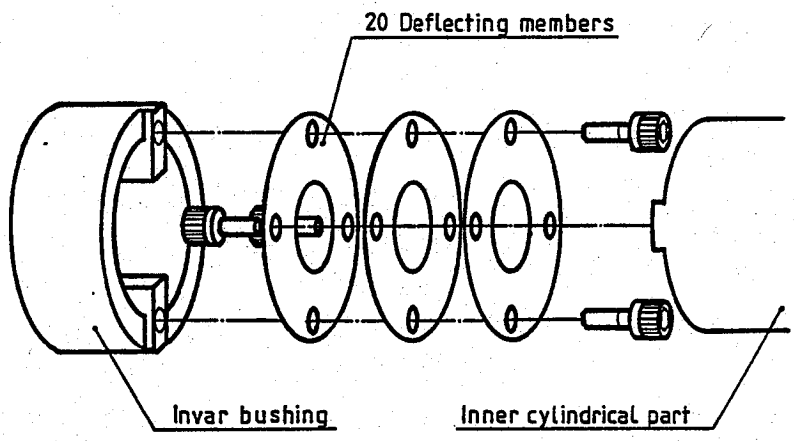

Fig. 23. Transverse support.

This solution permits the use of Invar as material for the bushing. The mirror surface deflections due to a thermal loading were determined to be ±4.5 nm which is very good.

3.2 3-Dimensional Model

A 3-D model is required to study the influence of the transverse support and the individual axial supports. The model describes 180 degrees of the mirror, thus enabling both the influence of transverse and axial supports to be studied by use of the same model.

The model has 2253 nodes, 36 Penta elements, 1632 Hexa8 elements and 156 Qaud4 elements. The Quad4 elements pave the surface of the mirror model. They are very thin elements with the sole purpose of providing a means for contour plotting and they do not interfere with the actual deformation calculations. The whole 3-D model is shown on figure 24 and the Quad4 elements that form the reflecting surface are shown on figure 25.

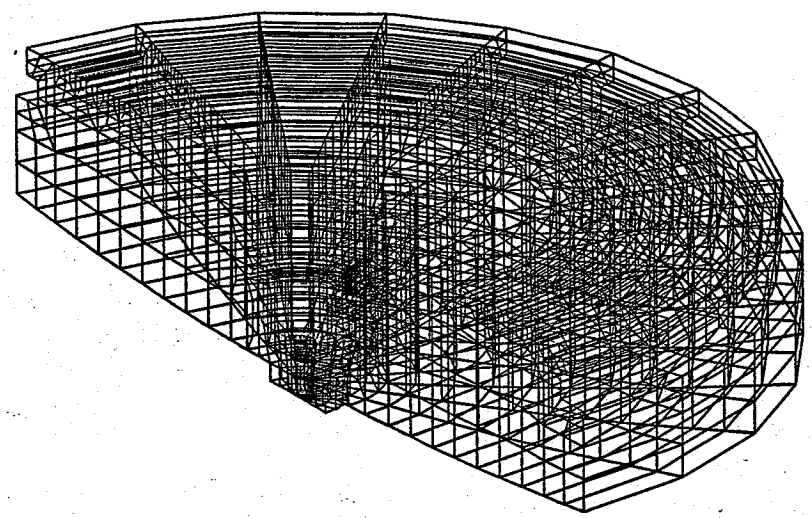

Fig. 24. 3-D finite element model of secondary mirror.

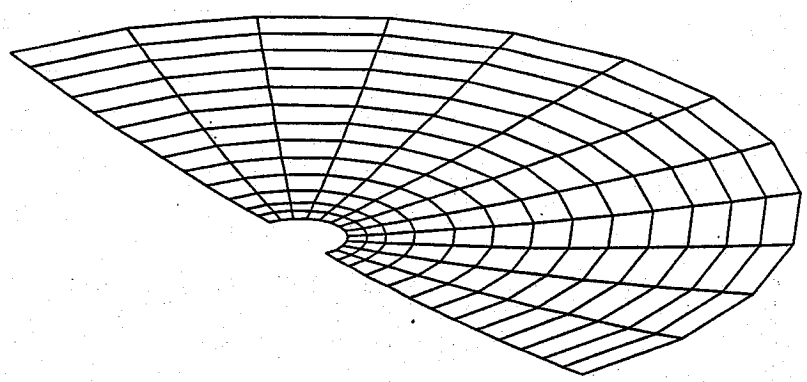

Fig. 25. Reflecting surface of the secondary mirror in the 3-D finite element model.

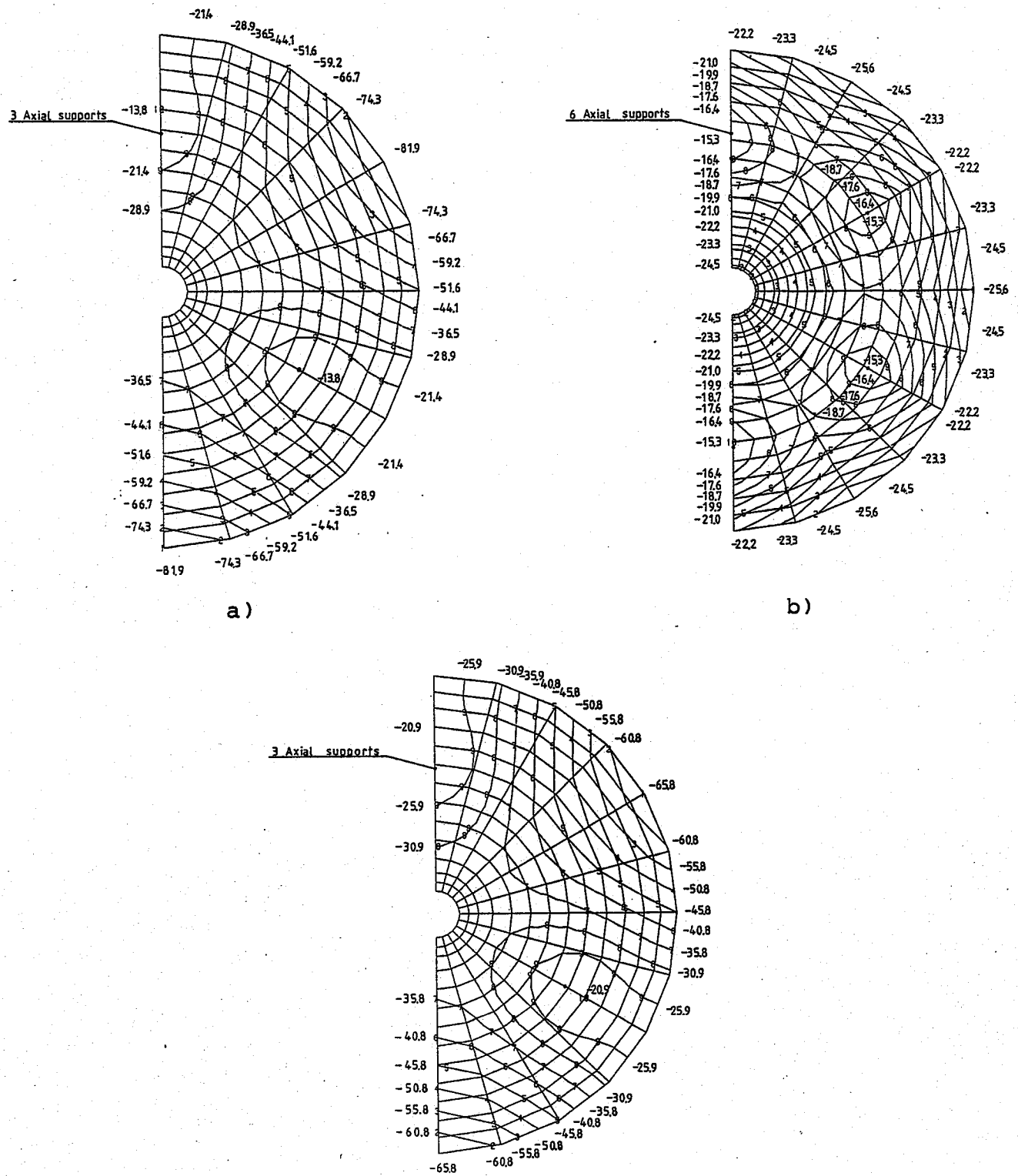

Fig. 27. Deflection patterns corresponding to the 3 suggested axial support configuration. Deflections are in nm.

The best solutions are 2 and 3. Solution 3 was chosen, since this solution is easier to implement mechanically and has fully acceptable displacements.

A workshop always works with certain manufacturing tolerances. The geometry of the axial support system will therefore not be exactly as described above, but will have small inevitable errors from manufacture. It is necessary to check that these errors in geometry do not lead to excessive deformation of the reflecting surface. Figure 28 shows the effect of minor errors in the support radius. The maximum surface displacements are shown corresponding to changes in the radius of the ring from 150 mm to 180 mm in steps of 5 mm. Figure 28 shows that a tolerance of about ±1 mm of the radius is fully acceptable.

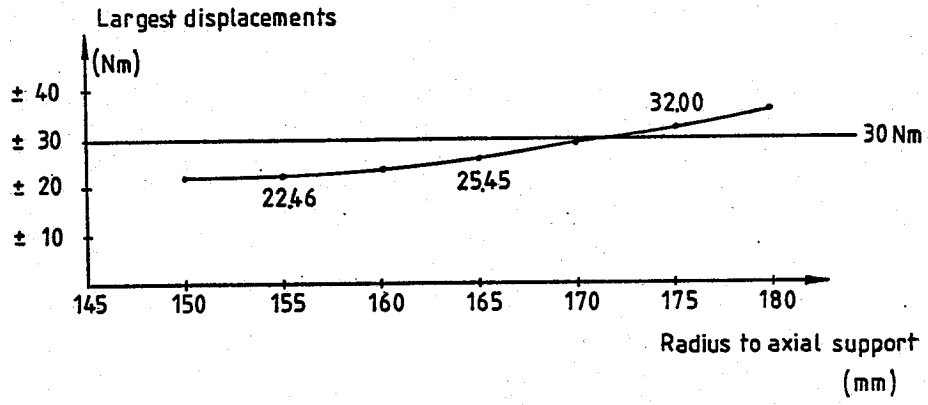

Fig. 28. Largest displacements as function of radius of axial support ring (3 fixed supports).

An error in the lateral position of the fixations of the "piano wires" to the cell will give forces and moments on the mirror (see figure 29).

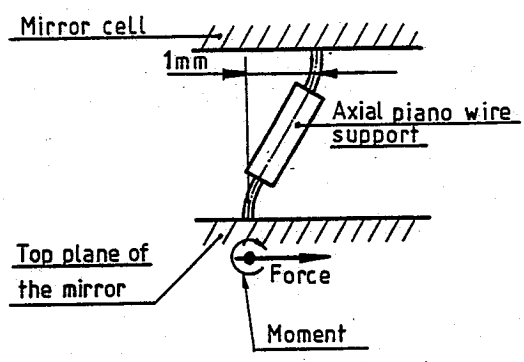

Fig. 29. Force and moment in mirror produced by a lateral shift of the fixation of the piano wire to the mirror cell.

To determine the necessary tolerances two cases have been studied.

1) Forces in radial direction (see figure 30a)

2) Forces all parallel (see figure 30b)

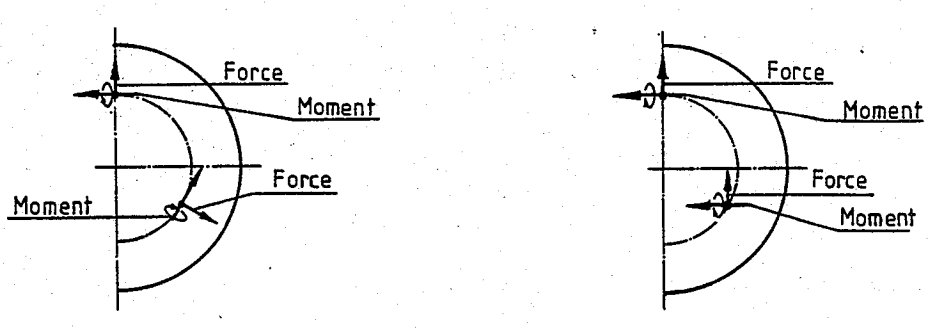

Fig. 30. Worst combination of forces and moments produced by lateral shift of supports in cell.

corresponding surface displacements are within ±2.3 nm, which is fully acceptable. (See figure 31).

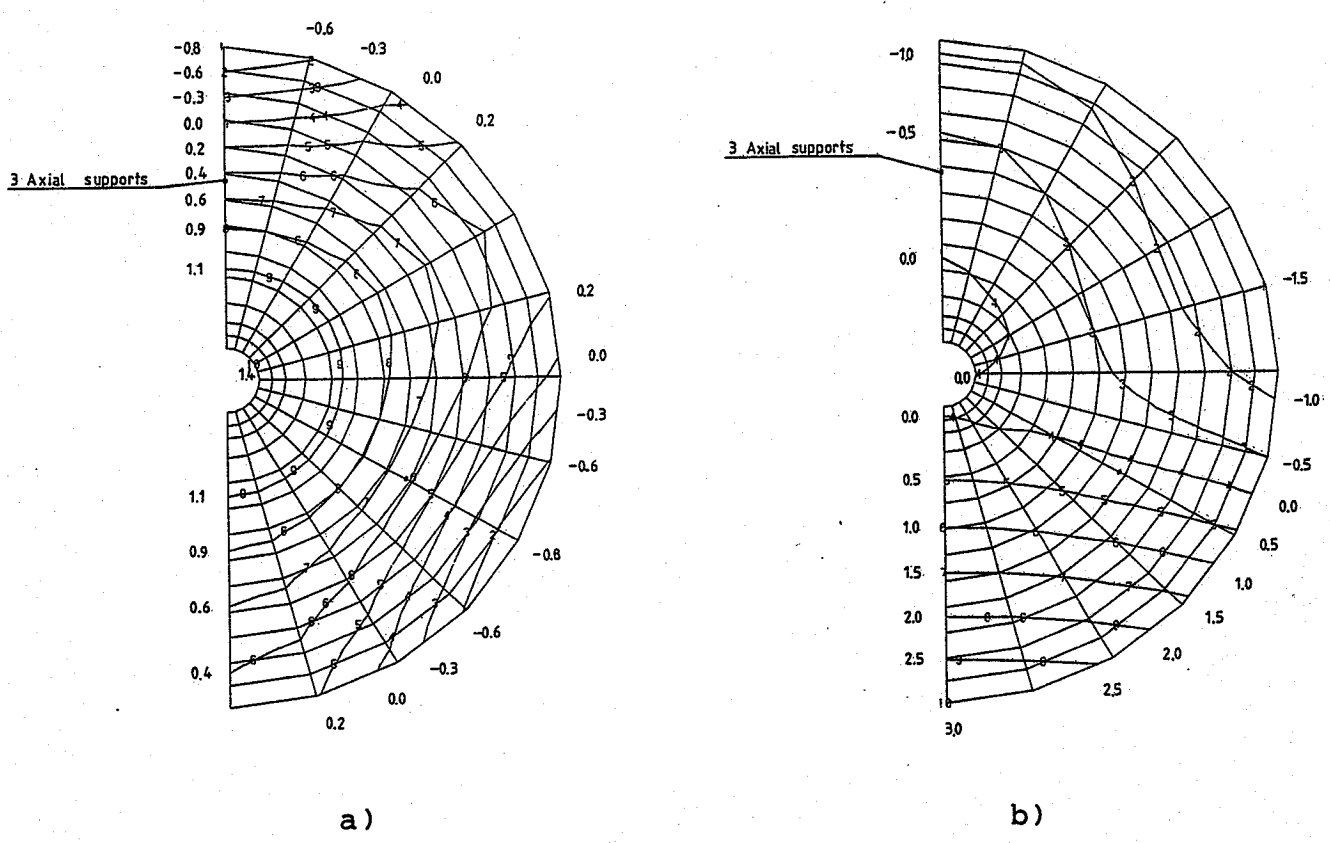

Fig. 31. Displacements (nm) from the load cases of figure 30.

Transverse Support. The transverse support system is placed in a hole in the center of the mirror. The support system has three main parts (see figure 23). An outer Invar-ring that is bonded to the mirror and an inner cylindrical part that is fixed to the mirror cell. To connect the Invar-ring and the inner cylindrical part there are 20-25 membranes.

To prevent this system from producing erroneous moments the membranes must be located in the plane of the center of gravity of the mirror.

When the transverse supports system carries the whole mirror load (telescope pointing to horizon), the displacements of the reflecting surface of the mirror are within ±6.1 nm which is acceptable (see figure 32).

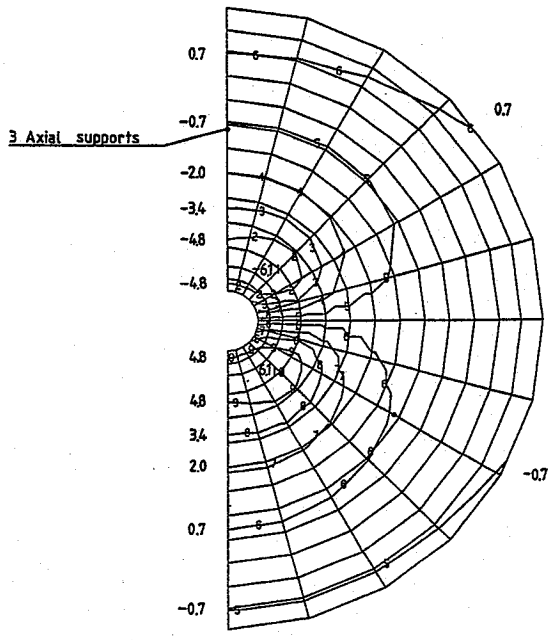

Fig. 32. Displacement (nm) of the reflecting surface due to transverse gravity load.

The secondary mirror can be tilted and displaced axially within its cell. This will give small forces and moments from the membranes in the transverse support system. The displacements due to these forces and moments have been determined and are acceptable (see figure 33).

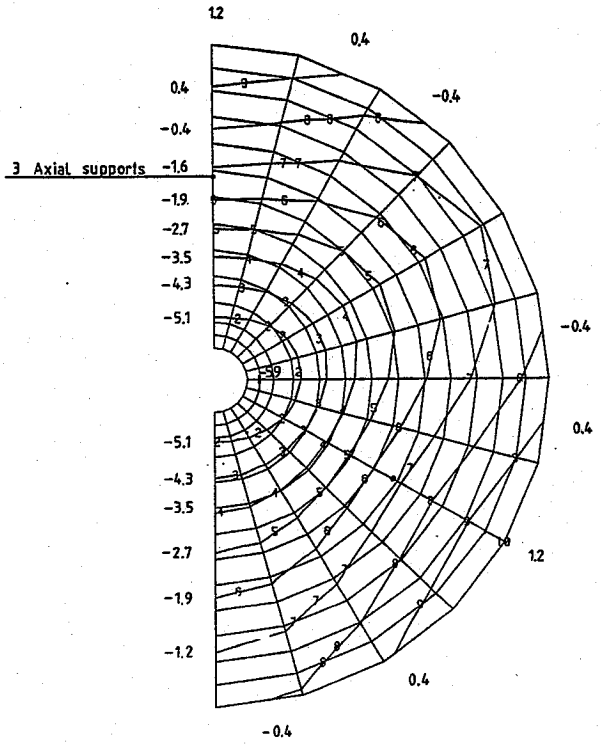

Fig. 33. Displacement (nm) produced by the transverse support system.

It is necessary to check that errors in geometry due to normal manufacturing tolerances will not lead to excessive surface deflections. An axial displacement of the transverse support will produce an axial force and a moment around a horizontal ring diameter. The effect of the force and the moment corresponding to an axial shift of 1 mm is shown in figure 34.

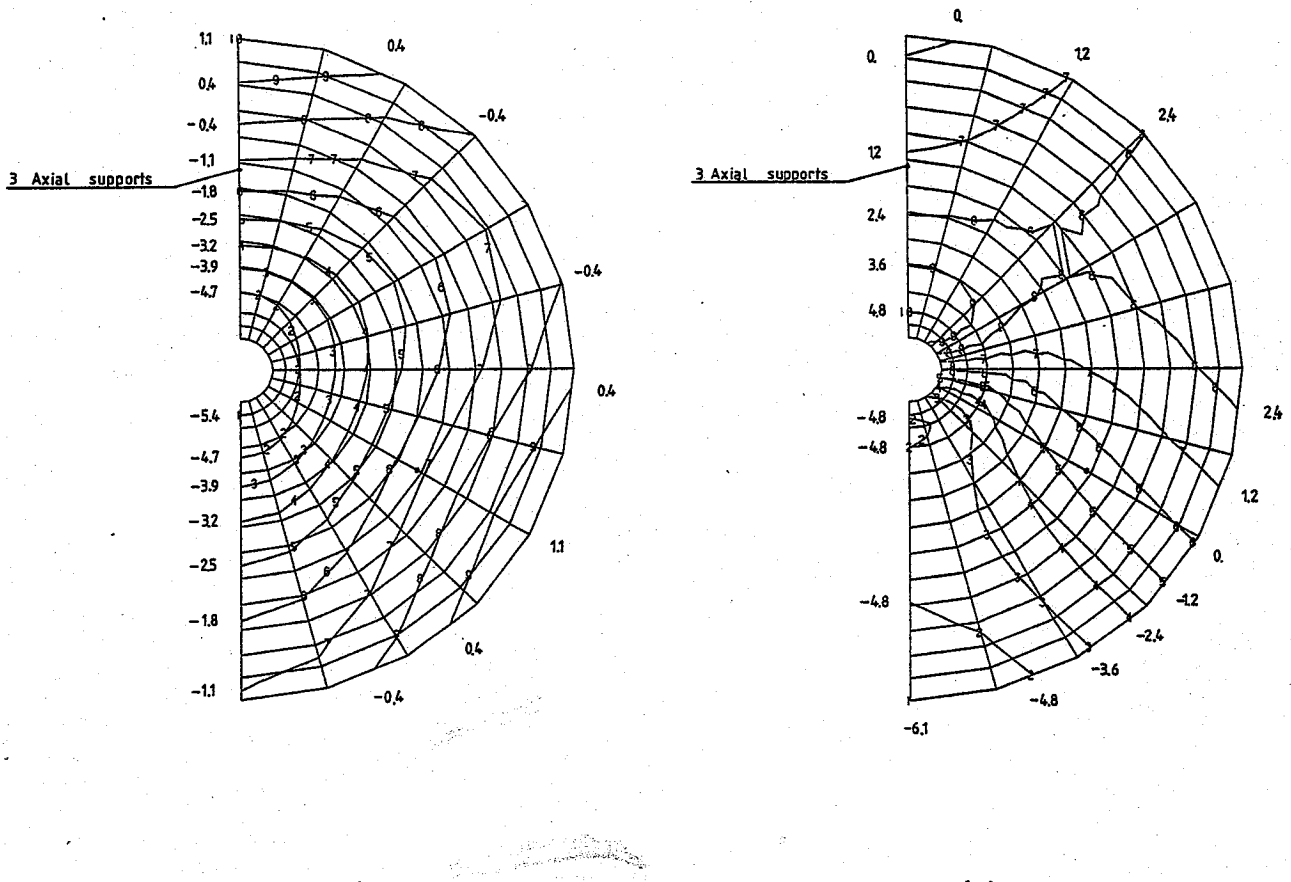

a) b)

Fig. 34. Displacement (nm) produced by forces (a) and moments (b) from transverse support.

The effect of the thermal expansion of the Invar ring was also checked with the 3-D model, since the thickness of the mirror has been increased after the axisymmetric model calculations. The new computation shows that the surface deformations are now smaller than with the previous thin mirror (see figure 35).

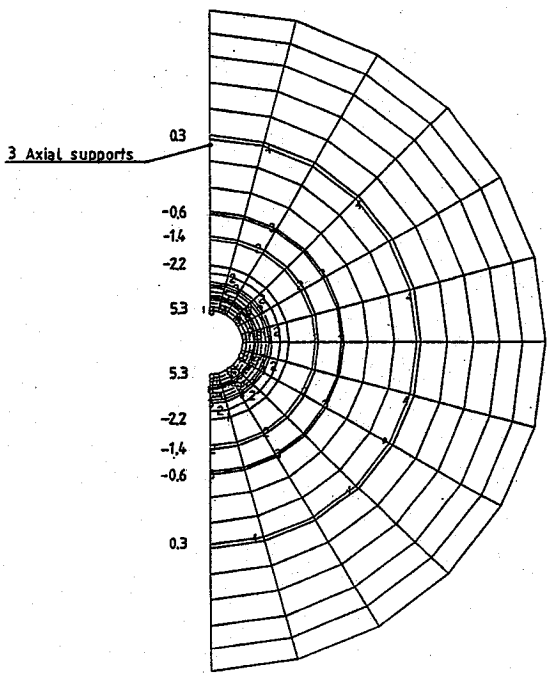

Fig. 35. Surface displacements (nm) caused by thermal expansion.

Combined Load. The image quality specification remains constant from zenith to an altitude of 30 degrees, from where it is relaxed. It is therefore of interest to study the combined load case corresponding to 30 degrees' altitude. The contour plot for this load case is shown on figure 36. The deflections are within ±11.9 nm. The deflection pattern is fully acceptable.

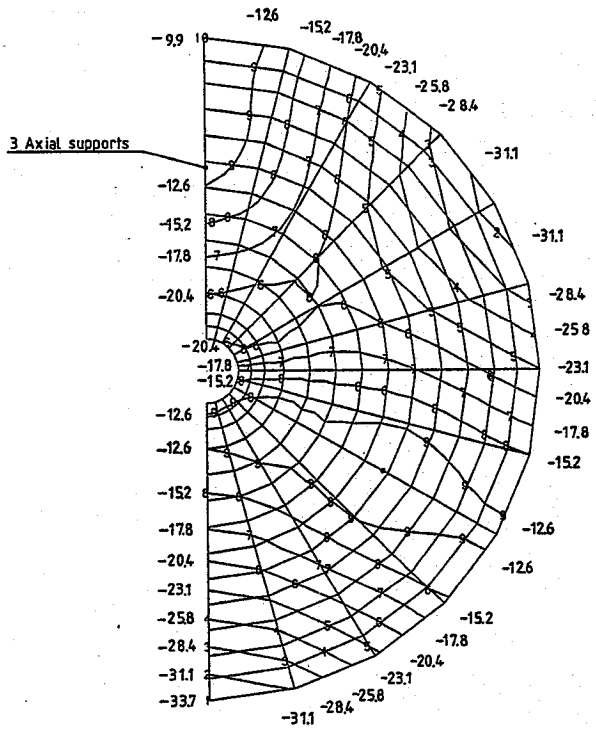

Fig. 36. Deflection pattern with telescope pointing to an altitude of 30 degrees. Deflections are in nm.

4. REFERENCES

(1) D.L. Crawford, A.B. Meinel and M.W. Stockton: A symposium on Support and Testing of Large Astronomical Mirrors. KPNO and University of Arizona, July 1968.

(2) B. Mack: Deflection and stress analysis of a 4.2 m diam primary mirror of an altazimuth-mounted telescope. Applied Optics, vol. 19, no 4, March 15, 1980.

(3) W. Siegmund: Deflection Analysis of a 3.5 m Homogenous Primary Mirror. Internal note from the MILT project group, March 1984.

(4) R. Richard and A. Malvick: Elastic Deformation of Lightweight Mirrors. Applied Optics, vol. 12, no 6, June 1973.

(5) R.H. MacNeal: MSC/NASTRAN, Handbook for Linear Static Analysis. The MacNeal-Schwendler Corporation, 1981.

Axial Supports. The 3-D model can be used to determine the required number of axial supports. There must be at least three supports to define the position of the mirror. These supports constitute the fixed points that establish a rigid connection between the mirror and its cell. Any excess supports are counterweighted lever arms.

For engineering reasons the number of supports should either be 3 or 6 (or more). Three configurations were studied:

1) A mirror disk with a height of 80 mm. 3 fixed axial supports.

2) A mirror disk with a height of 80 mm. 3 fixed axial supports and 3 counterweighted lever arms.

3) A mirror disk with a height of 100 mm. 3 fixed axial supports.

The results of the calculations related to the 3 above solutions are given in figure 26.

Solution	Disk thickness	Fixed axial supports	Counterweighted lever arms	Optimal support ring radius	Displacements at the reflecting surface	Figure
1	80 mm	3		155 mm	± 34 nm	27 a
2	80 mm	3	3	165 mm	± 5 nm	27 b
3	100 mm	3		155 mm	± 22.5 nm	27 c

Fig. 26. Results from axial support calculations.

From the results it can be seen that the optimal support radius using three fixed axial supports and three counterweighted levers is equal to the one determined with the axisymmetric model described in 3.1.